

# Comparison of Structural Types of L-Alanine Pentamer by Quantum Chemical Calculation

Minoru Kobayashi and Jae Ho Sim<sup>\*,†</sup>

Graduate School of Bio-Applications and Systems Engineering, Tokyo University of Agriculture and Technology,  
Tokyo 184-8588, Japan

<sup>\*</sup>Department of Advanced Materials & Chemical Engineering, Halla University, Wonju 26404, Korea  
(Received July 1, 2022; Revised July 20, 2022; Accepted July 21, 2022)

## Abstract

L-alanine (LA, as an amino acid residue) pentamer model was used to investigate changes in the dihedral angle, intramolecular hydrogen bonding and formation energies during structural optimization. LA pentamers having four conformation types [ $\beta$ :  $\varphi/\psi=t-t+$ ,  $\alpha$ :  $\varphi/\psi=g-g-$ , PP<sub>II</sub>:  $\varphi/\psi=g-t+$  and P-like:  $\varphi/\psi=g-g+$ ] were carried out by quantum chemical calculations (QCC) [B3LYP/6-31G(d,p)]. In LA,  $\beta$ ,  $\alpha$ , and P-like types did not change by optimization, having an intra-molecular hydrogen bond: NH $\cdots$ OC (H-bond), and PP<sub>II</sub> types in the absence of H-bond were transformed into P-like at the designated  $\psi$  of 140°, and to  $\beta$  at that of 160° or 175°. P-like and  $\alpha$  were about 0.5 kcal/mol/mu more stable than  $\beta$ . In order to understand the processes of the transformations, the changes of  $\varphi/\psi$ , distances of NH-OC ( $d_{\text{NH/CO}}$ ) and formation energies ( $\Delta E$ , kcal/mol/mu) were examined.

**Keywords:** Conformation, Oligopeptide, Alanine, Pentamer, Quantum chemical calculation

## 1. Introduction

Understanding conformation of oligopeptide is important because the conformation often reflects the chain propagation and folding process, and decides the fundamental properties such as stability and activity.

Many experimental and theoretical studies concerning the conformations of oligopeptides have been reported[1,2]. L-Alanine is widely distributed in nature in the free state as well as a constituent of proteins. As for alanine oligomers, for example, Marqusee *et al.* investigated the structure of alanine 16-mer by CD and reported that  $\alpha$ -helical conformation (hereinafter referred to as  $\alpha$ ) was stable in aqueous state[3]. Eker *et al.* studied the Raman, FTIR, and CD spectra of alanine trimer in water and postulated that the trimer existed as a 50:50 mixture of polyproline II helix (hereinafter referred to as PP<sub>II</sub>) and extended  $\beta$ -strand-like conformation (hereinafter referred to as  $\beta$ )[4,5]. Shi *et al.* found from <sup>1</sup>H-NMR spectrum that alanine heptamer dominantly possessed polyproline II helix conformation[6]. Woutersen *et al.* studied the Two-Dimensional Spectroscopy of trialanine and molecular dynamics (MD) simulation[7,8]. Graf *et al.* studied the <sup>1</sup>H-NMR spectrum of alanine trimer and reported that it had 90% of PP<sub>II</sub> and 10% of  $\beta$ -extended structures[9].

Concerning theoretical calculation studies of alanine oligomers, Mu

*et al.* calculated the conformational population of trimer in aqueous state using molecular mechanics method reported that the main conformation was PP<sub>II</sub>[10]. Kentsis *et al.* obtained similar results for 7- and 14-mers using the Monte Carlo method[11]. Bour *et al.* studied the aqueous effects using the conductor-like screening solvent model (COSMO), appropriate for water, and found that a helix conformation was stable[12].

The conformational populations of alanine oligomers reported, as mentioned above, have been different with conditions such as sequence lengths, gaseous or aqueous state, experimental or computational methods, and so on.

We have investigated the structural type of gaseous and hydrated alanine oligomer models by incorporating the quantum chemical calculation (QCC). In our previous study[13], we found that alanine heptamer has three stable conformers of shrunken polyproline II (hereinafter referred to as P-like),  $\alpha$ -helical (hereinafter referred to as  $\alpha$ -helix), and extended  $\beta$ -strand-like (hereinafter referred to as  $\beta$ -extended) conformation, in the order of stability, by convergent calculation starting from alanine dimer models using quantum chemical calculation (QCC).

In this paper, in order to deepen the understanding of conformations of oligopeptide, the conformations of oligopeptide having amino acid residues were studied by QCC. Using L-alanine (as an amino acid residue) pentamer model, the changes of dihedral angles ( $\varphi/\psi$  values), intra-molecular hydrogen bonds and formation energies in the structure optimization processes were examined.

<sup>†</sup> Corresponding Author: Halla University  
Department of Advanced Materials & Chemical Engineering, Wonju 26404, Korea  
Tel: +82-33-760-1494 e-mail: jhsim@halla.ac.kr

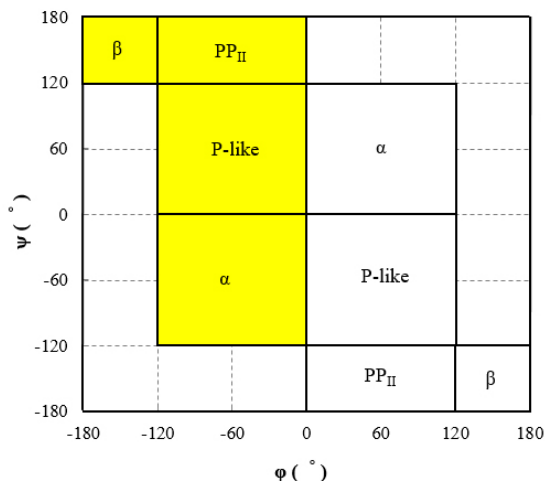
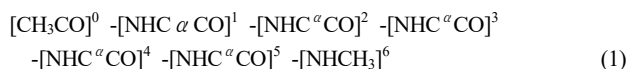


**Figure 1.** Four conformation types ( $\varphi/\psi$ ). The  $\beta$  ( $\beta$ -extended:  $t/t+$ ),  $PP_{II}$  ( $g/t+$ ), P-like ( $g/g+$ ) and  $\alpha$  ( $\alpha$ -helix:  $g/g-$ ) with yellow marks were used in designations.

## 2. Quantum chemical calculations (QCC)

### 2.1. Calculation models

The L-alanine (LA) pentamer model ( $CH_3CO-[NHCH(CH_3)CO]_5-NHCH_3$ ), molecular weight 428.56) used in this study. Acetyl ( $CH_3CO-$ ) and methyl amino ( $-NHCH_3$ ) groups were used as end groups of amino (N-end) and carboxyl (C-end) terminals, respectively. Formula (1) shows the molecular units of LA as an example.



Where,  $n$  ( $n = 0 - 6$ ) shows the position of sequence units.

In designations of LA, four conformation types ( $\beta$ -extended:  $\varphi/\psi = t-t+$ ,  $\alpha$ -helix:  $g-g-$ ,  $PP_{II}$ :  $g-t+$  and P-like:  $g-g+$ ) were used as shown in Figure 1. The  $\varphi_n/\psi_n$  is the combinations of dihedral angles ( $\tau_n$ ) repeated for the unit of  $CN-C^{\alpha}C/NC^{\alpha}-CN$  bonds. The conformations were specified based on the IUPAC rule[14] as follows:  $\tau_n$  of trans ( $t\pm$ ) and gauche ( $g\pm$ ) are  $\pm 120^\circ$  to  $\pm 180^\circ$  and  $\pm 0^\circ$  to  $\pm 120^\circ$ ,

respectively. The types of  $\varphi_n/\psi_n$  ( $n = 5$ ) were specified as follows: trans and gauche types are ( $t/t$ ) and ( $g/t$ ,  $t/g$ , or  $g/g$ ), respectively, using the average value of  $\varphi_n/\psi_n$  ( $n = 1-5$ ). As designated values of  $(\chi_n/\varphi_n/\psi_n)_{n=1-5}$  of  $\beta$ -extended, P-like, and  $\alpha$ -helix, the values obtained for pentamers by convergent calculation from alanine dimer model were used[11]. For the  $(\chi_n/\varphi_n/\psi_n)_{n=1-5}$  value of  $PP_{II}$ , the values of three kinds ( $\varphi_n/\psi_n = -60/140^\circ$  reported by Graf, *et al.*[9],  $-60/160^\circ$  and  $-60/175^\circ$ ) were used. The designated  $\varphi_n/\psi_n$  values are shown in Table 1.

### 2.2. Structure optimizations

The comparison of structure types (structure optimizations) were then carried out by quantum chemical calculation method (QCC). The "Gaussian 03W" (Gaussian Inc.) software was used[15]. In the structural optimizations for LA, B3LYP as a density functional theory (DFT) was used with the self-consistent field (SCF) method. 6-31G(d,p) (d,p: polarization) was used as a basis set. Energies (E: HF, 1 Hartree = 627.51 kcal/mol) and structural parameters such as dihedral angle, molecular length and hydrogen bond length were obtained from the optimized structures.

The conformations were specified as mentioned in the calculation models section. Molecular length was defined by  $L(\text{\AA})$ , where the  $L$  is non-bonding distance between N atom in N-end and C atom in C-end (CO). The formation of hydrogen bond(H-bond) distance was confirmed by the NH-CO distances with reference(2.74  $\text{\AA}$  in regular ice[16], 2.85  $\text{\AA}$  in liquid[16], and 2.98  $\text{\AA}$  in vapor[17, 18]). The NH-CO distances [ $d_{NH/CO}$  ( $\text{\AA}$ )] of H-bond were shorter than 2.30 $\text{\AA}$ , and those having no H-bond were longer than 2.7 $\text{\AA}$ , according to the calculated results. Add a diagram representing discussed angles and distances used in this structure optimization.

## 3. Results and discussion

L-alanine pentamer (LA, as an amino acid residue) models, each having four conformation types [ $\beta$ -extended:  $\varphi/\psi = t-t+$ ,  $\alpha$ -helix:  $g-g-$ ,  $PP_{II}$ :  $g-t+$  and P-like:  $g-g+$ , see Figure 1] were compared with various structure types by the QCC methodology, and the optimized structure and formation energy were examined for each des-

**Table 1.** Structure Optimization Result for L-alanine Pentamer (LA)<sup>a</sup>

Designated type ( $\varphi/\psi$ , $^\circ$ )	Optimized type ( $\varphi/\psi$ , $Av^\circ$ )	Number of intra-molecular H-bond		Dipole moment $\mu$ (Debye) <sup>b</sup>	Molecular length: $L(\text{\AA})^c$	Formation energy	
		$N_{NH/CO}$	( $d_{NH/CO}$ , $\text{\AA}$ )			E (HF)	$\Delta E_\beta^d$ (kcal/mol/mu)
$\beta$ (-160/164)	$\beta_1$ (-156/163)	5	(2.15 - 2.18)	4.88	16.72	-1485.2890	0.00
$\alpha$ (-72/-14)	$\alpha$ (-73/-13)	4	(2.15 - 2.25)	7.91	10.24	-1485.2927	-0.48
P-like (-85/69)	P-like (-84/56)	5	(2.02 - 2.04)	4.46	13.85	-1485.2930	-0.50
$PP_{II}$ (-60/140)	P-like (-85/68)	5	(2.02 - 2.04)	4.47	13.85	-1485.2930	-0.50
$PP_{II}$ (-60/160)	$\beta_2$ (-141/145)	5	(2.16 - 2.30)	2.65	16.32	-1485.2883	0.09
$PP_{II}$ (-60/175)	$\beta_2$ (-141/145)	5	(2.16 - 2.30)	2.64	16.34	-1485.2883	0.09

<sup>a</sup> Calculated by B3LYP/6-31+G(d,p). <sup>b</sup>  $\mu = (\mu_x^2 + \mu_y^2 + \mu_z^2)^{1/2}$ .

<sup>c</sup> The  $L$  is non-bonding distance between N atom in N-end (NH) and C atom in C-end (CO).

<sup>d</sup> The  $\Delta E_\beta$  values were calculated based on the energy of  $\beta_1$  structure.

igned structure. In our previous studies[19], as mentioned in the introduction section, the PP<sub>II</sub> type designated for LA transformed into P-like(or  $\alpha$ -helix) and  $\beta$ -extended type, respectively, in each optimization. Therefore, these designations for LA were carried out in detail using three  $\psi$  values ( $t^+$ ) of 140, 160 and 175°.

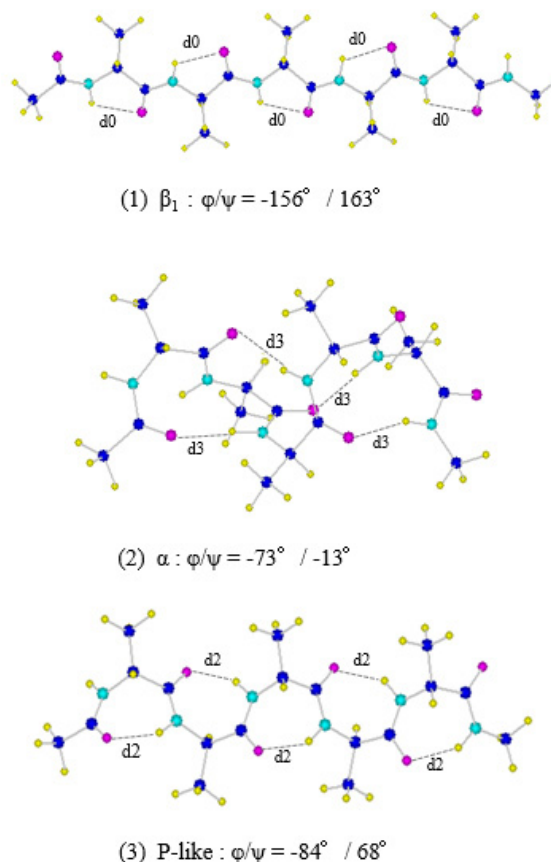
### 3.1. Optimized structure and energy

Table 1 lists the optimized Result for LA. The number of intra-molecular hydrogen bonds between peptide groups (NH/CO), (hereinafter referred to as H-bond) are shown as  $N_{\text{NH/CO}}$ . There were two groups of NH-CO distance (hereinafter referred to as  $d_{\text{NH/CO}}$ ); shorter than 2.3Å (H-bond) and longer than 2.7Å (no H-bond), according to the calculated results. In this study,  $d_{\text{NH/CO}}$  is classified by the number of amino acid units between the NH/CO groups and named as dn: for example, d0 indicates the NH-CO distance in the same amino acid, d1 indicates the neighboring units. The amino acid position is indicated in the parenthesis. The formation energy difference ( $\Delta E_{\beta}$ , kcal/mol/mu, mu: monomer unit) was calculated based on E value of  $\beta_1$  optimized for  $\beta$  type.

The models designated with  $\beta$ ,  $\alpha$ , and P-like were each optimized into the same conformation type as those designated. However, the models designated with PP<sub>II</sub> were transformed into other types; P-like in the designated  $\psi$  of 140° and  $\beta_2$  in those of 160 and 175°. It is noteworthy that the transformed conformation types differed, depending on the designated dihedral angles. P-like obtained from PP<sub>II</sub> type designated with  $\psi$  of 140° was the same as those of P-like from P-like type. PP<sub>II</sub> type designated with  $\psi$  of 160 and 175° were transformed into  $\beta$  ( $\beta_2$ ) type, which is slightly different from  $\beta_1$  from designated  $\beta$  type: in dihedral angle ( $\varphi/\psi$ ), molecular length (L) and dipole moment ( $\mu$ ), except for  $N_{\text{NH/CO}}$ . This result indicates that the H-bond formation types differ with those of  $\beta_1$  and  $\beta_2$ , as described later in detail. It is also notable that the optimized structures having the same conformation type differ, depending on designation of various conformation types.

The (1), (2) and (3) in Figure 2 depict the conformations of  $\beta_1$ ,  $\alpha$  and P-like optimized for the model of LA of  $\beta$ ,  $\alpha$  and P-like, respectively. There were three types of H-bonds in this study; H-bond in the same amino acid unit (hereinafter d0 type H-bond), between the amino acid units with one (hereinafter d2 type H-bond) and two (hereinafter d3 type H-bond) separated units. The  $\beta_1$  had five H-bonds having 5-membered rings between peptide groups in the same units (d0 type H-bond). The  $\alpha$  had four H-bonds having 10-membered rings between peptide groups in which two units were separated (d3 type H-bond). The P-like had five H-bonds having 7-membered rings between peptide groups in which one unit was separated (d2 type H-bond). It is interesting that in  $\alpha$  and P-like the end groups formed d3 and d2 type H-bonds, respectively, although in  $\beta_1$  no end group formed H-bond.

Figure 3 depicts the designated [PP<sub>II</sub>:  $\varphi/\psi = -60 / 160^\circ$ , (1)] and optimized [ $\beta_2$ , (2)] structures for PP<sub>II</sub> model of LA. Three groups of  $d_{\text{NH/CO}}$ : d0, d1 and d2 were read out. The d0, d1 and d2 values of designated PP<sub>II</sub> were in the range of 3.46 - 3.59, 5.57 - 5.66 and 4.18 -



**Figure 2.** Optimized structures of  $\beta_1$  (1),  $\alpha$  (2) and P-like (3) of LA. The d0, d2, and d3: distances ( $d_{\text{NH/CO}}$ ) between NH/CO groups in the same units, and the units with one and two separated units, respectively. (- -) : H-bond.

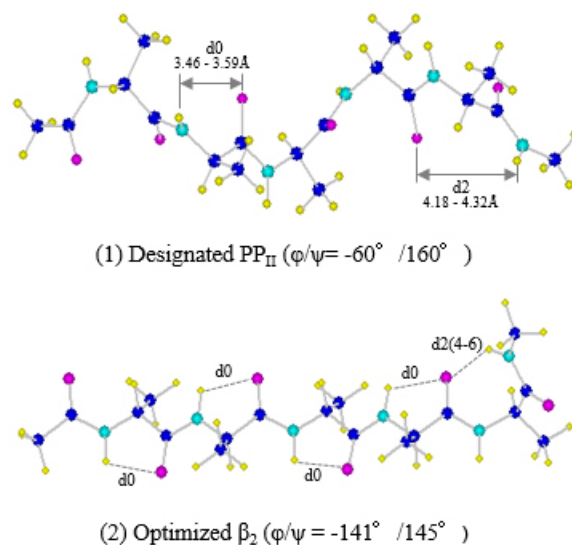


**Figure 3.** Designated PP<sub>II</sub> (1) and optimized  $\beta_2$  (2) structures of LA. In (2), d0 was 2.16 - 2.18Å and d2 was 2.18Å.

4.32Å, respectively, indicating that no H-bonds were formed. On the other hand, the optimized  $\beta_2$  had four d0 type H-bonds ( $d_0 = 2.16$

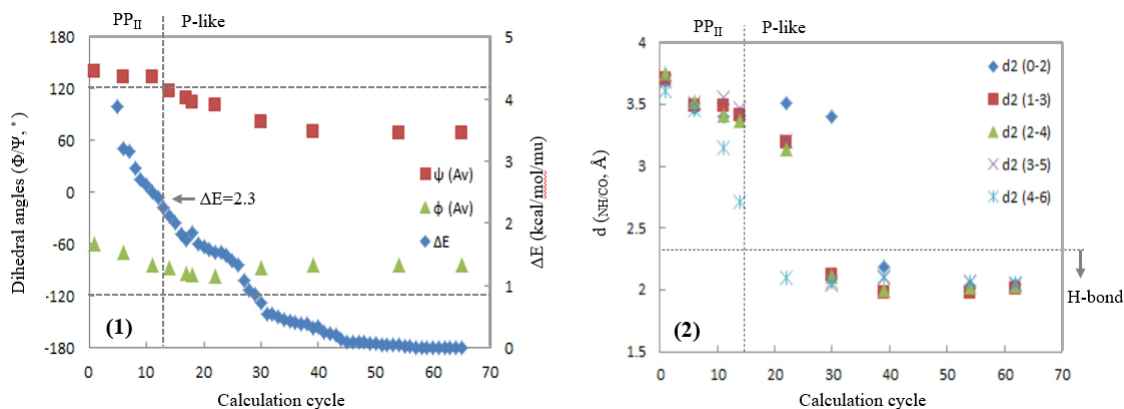


**Figure 4.** Structure optimization process of LA designated with PP<sub>II</sub> ( $\varphi/\psi = -60^\circ/140^\circ$ ). The designated structure was transformed into P-like ( $\varphi/\psi = -85^\circ/68^\circ$ ). (1)  $\varphi/\psi$  (Av) and  $\Delta E$  values.  $\Delta E$  at 0 cycle: 70.7 kcal/mol/mu ( $E_0 = -1484.7298$  HF). (2)  $d_{\text{NH/CO}}$ , d2 : between NH/CO groups separated by one unit.

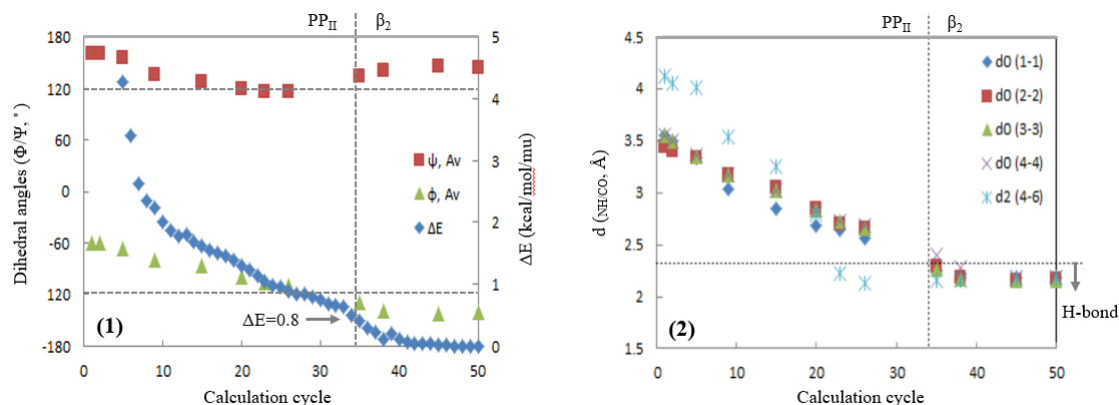


**Figure 5.** Structure optimization process of LA designated with PP<sub>II</sub> ( $\varphi/\psi = -60^\circ/160^\circ$ ). The designated structure was transformed into  $\beta_2$  ( $\varphi/\psi = -141^\circ/145^\circ$ ). (1)  $\varphi$ ,  $\psi$  (Av) and  $\Delta E$  values.  $\Delta E$  at 0 cycle: 72.3 kcal/mol/mu ( $E_0 = -1484.7124$  HF). (2)  $d_{\text{NH/CO}}$ , d0 : between NH/CO groups in the same unit.

- 2.18Å) and one d2 type H-bond [ $d_2 = 2.18\text{Å}$ , between CO in 4-th unit and NH in C-end (hereinafter  $d_2(4-6)$ ). The most distinctive differences between  $\beta_1$  and  $\beta_2$  were the number and kinds of H-bond types;  $\beta_1$  had five d0 type H-bonds and  $\beta_2$  had four d0 type and one d2 type H-bonds, resulting from the difference of designated  $\varphi$  values between  $\beta_1$  ( $\varphi = -160^\circ$ ) and  $\beta_2$  ( $\varphi = -140^\circ$ ). The structure of P-like optimized for PP<sub>II</sub> type having  $\varphi/\psi$  values of  $-60/140^\circ$  was the same as that of P-like optimized for P-like type [see (3) in Figure 2].

### 3.2. Optimization process

The conformations of LA designated with PP<sub>II</sub> were transformed into P-like or  $\beta$  ( $\beta_2$ ). Therefore, in order to understand the processes of such conformational transformations, their optimization processes were examined in detail. Figures 4, 5 and 6 depict the results for the processes of optimizations for the designated  $\psi$  values of 140, 160 and 175°, respectively. In each figure, (1) shows the changes of averaged dihedral angles [ $\varphi_n$  and  $\psi_n$ ,  $n=1-5$ , °] and formation energies ( $\Delta E$ : the formation energy difference between the optimized structure and structure of optimization process, kcal/mol/mu), and (2) shows the

changes of  $d_0$  or  $d_2$  ( $n = 1-5$ , Å). The broken line in each figure shows the boundary between the designated and optimized conformation types (see Figure 1).

As shown in (1) of Figure 4 (designated with PP<sub>II</sub>:  $\varphi/\psi = -60/140^\circ$ ),  $\psi$  values decreased with optimization cycle, and PP<sub>II</sub> was transformed into P-like ( $\varphi/\psi = -88 \sim -84/120^\circ$ ) at 11 to 14 cycles. The  $\varphi/\psi$  value of optimized P-like conformer was  $-85/68^\circ$  (63 cycles). The  $d_2$  values in (2) largely decreased with decreases of  $\psi$  values, and P-like had d2 type H-bond ( $d_2 \text{ Av} = 2.03 - 2.35\text{Å}$ ) after 30 cycles. The  $d_2(4-6)$  values significantly decreased from the early cycles, compared to internal  $d_2$  values. This decrease in speed indicates that the C-end was more mobile, and the N-end was less mobile, while the internal units had intermediate mobility.

On the other hand, as shown in (1) of Figure 5 (designated with PP<sub>II</sub>:  $\varphi/\psi = -60/160^\circ$ ),  $\varphi$  values decreased with optimizations, and PP<sub>II</sub> was transformed into  $\beta$  ( $\varphi/\psi = -120/120 - 134^\circ$ ) at 26 to 35 cycles. The  $\varphi/\psi$  value of optimized  $\beta$  conformer was  $-141/145^\circ$  (50 cycles). The  $d_1$  values in (2) decreased with decreases of  $\varphi$  values, and  $\beta$  had d1 type H-bond ( $d_1 \text{ Av} = 2.30\text{Å}$ ) at 45 to 55 cycles.

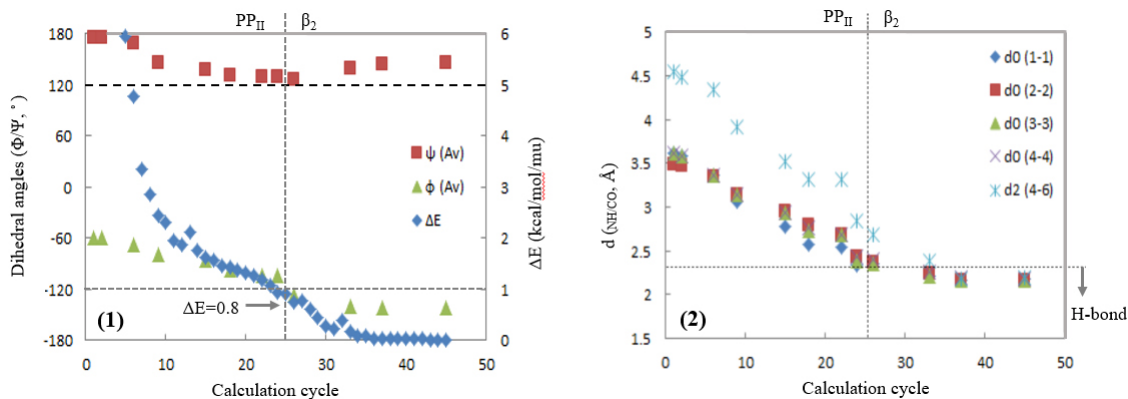


**Figure 6.** Structure optimization process of LA designated with PP<sub>II</sub> ( $\phi/\psi = -60^\circ/175^\circ$ ). The designated structure was transformed into  $\beta_2$  ( $\phi/\psi = -141^\circ/145^\circ$ ). (1)  $\phi/\psi$  (Av) and  $\Delta E$  values.  $\Delta E$  at 0 cycle: 75.2 kcal/mol/mu ( $E_0 = -1484.6888$  HF). (2)  $d_{\text{NH/CO}}$ .  $d_0$ : between NH/CO groups in the same unit.

The d2(4-6) values largely decreased from early cycles as in the case of Figure 4, compared with internal  $d_0$  values, and finally  $\beta_2$  had d2(4-6) type H-bond. The optimization processes in the case of designated  $\psi$  of  $175^\circ$  [(1) and (2) of Figure 6], were almost the same as those shown in Figure 5.

The formation energies ( $\Delta E$ ) at initial points (calculation cycle = 0) of three designated structures (PP<sub>II</sub>:  $\psi = 140, 160$ , and  $175^\circ$ ), as shown in the captions of (1) of Figures 4-6, were 71, 72, and 75 kcal/mol/mu, respectively. The  $\Delta E$  in the transformation points at designated  $\psi$  of  $140$  and  $160 - 175^\circ$ , as shown in (1) of Figures 4-6, were 2.3 and 0.8 kcal/mol/mu, respectively. These results indicate that the formation energies at initial and transformation points were affected by the designated  $\psi$  values.

#### 4. Conclusion

The comparison between the conformations of oligopeptides having amino acid residues was studied by QCC. In L-alanine pentamer (LA) having amino acid residues, the P-like and  $\alpha$  conformers having intra-molecular hydrogen bonds (H-bonds) were stable, and the PP<sub>II</sub> conformer having no H-bond was not obtained. Furthermore, the PP<sub>II</sub> designated for LA was transformed into P-like or  $\beta$  dependently of the designated  $\psi$  values.

It was found that the effects of amino acid residues on the conformational transformations were attributed to the presence or absence of amino proton in the amino acid residue, and the conformational transformation of oligopeptide having amino acid residue was strongly affected by the intra-molecular hydrogen bonding between the main chain and the C-end having NH group, simultaneously by intra-molecular hydrogen bonding between the main chain.

#### Acknowledgment

This research was supported by Halla University academic research fund, 2022.

#### References

1. B. Yogeswari, R. Kanakaraju, S. Boopathi, and P. Kollandaivel, Combined theoretical studies on solvation and hydrogen bond interactions in glycine tripeptide, *Mol. Simul.*, **40**, 942-958 (2013).
2. V. Parchansky, J. Kapitan, J. Kaminsky, J. Sebestick, and P. Bour, Ramachandran plot for alanine dipeptide as determined from Raman optical activity. *J. Phys. Chem. Lett.*, **4**, 2763-2768 (2013).
3. S. Marqusee, V. H. Robbins, and R. L. Baldwin, Unusually stable helix formation in short alanine-based peptides, *Proc. Natl. Acad. Sci., USA*, **86**, 5286-5290 (1989).
4. F. Eker, X. Cao, L. Nafie, and R. Schweitzer-Stenner, Tripeptides adopt stable structures in water. A combined polarized visible Raman, FTIR, and VCD spectroscopy study, *J. Am. Chem. Soc.*, **124**, 14330-14341 (2002).
5. F. Eker, K. Griebenow, and R. Schweitzer-Stenner, Stable conformation of tripeptides in aqueous solution studied by UV circular dichroism spectroscopy, *J. Am. Chem. Soc.*, **125**, 8178-8185 (2003).
6. Z. Shi, C. A. Olson, G. D. Rose, R. L. Baldwin, and N. R. Kallenbach, Polyproline II structure in a sequence of seven alanine residues, *Proc. Natl. Acad. Sci., USA*, **99**, 9190-9195 (2002).
7. S. Woutersen and P. Hamm, Structure determination of trialanine in water using polarization sensitive two-dimensional vibrational spectroscopy, *J. Phys. Chem. B*, **104**, 11316-11320 (2000).
8. S. Woutersen, R. Pfister, P. Hamm, Y. Mu, D. S. Kosov, and G. Stock, Peptide conformational heterogeneity revealed from non-linear vibrational spectroscopy and molecular-dynamics simulations, *J. Chem. Phys.*, **117**, 6833-6840 (2002).
9. J. Graf, P. H. Nguyen, G. Stock, and H. Schwalbe, Structure and dynamics of the homologous series of alanine peptides: A joint molecular dynamics/NMR study, *J. Am. Chem. Soc.*, **129**, 1179-1189 (2007).
10. Y. Mu, D. S. Kosov, and G. Stock, Conformational dynamics of trialanine in water. 2. Comparison of AMBER, CHARMM, GROMOS, and OPLS force fields to NMR and infrared experiments, *J. Phys. Chem. B*, **107**, 5064-5073 (2003).
11. A. Kentsis, M. Mezei, T. Gindin, and R. Osman, Unfolded state of polyalanine is a segmented polyproline II helix, *Proteins: Struct. Funct. Bioinf.*, **55**, 493-501 (2004).

12. P. Bour, J. Kubelka, and T. A. Keiderling, Ab initio quantum mechanical models of peptide helices and their vibrational spectra, *Biopolymers.*, **65**, 45-49 (2002).
13. M. Kobayashi, J. H. SIM, and H. Sato, Conformational analyses for alanine oligomer during chain propagation by quantum chemical calculation, *Polymer J.*, **47**, 369-378 (2015).
14. J. Rigaudy and S. P. Klesney, *Nomenclature of Organic Chemistry: Section E*, 483, Oxford Pergamon Press (1979).
15. M. J. Frish, G. W. Truck, H. B. Schlegel, and G. E. Scuseria, Gaussian 03 User's Reference, *Manual version*, Gaussian Inc., Carnegie, PA, 15106 USA, (2003).
16. R. Ludwig, Water from cluster to the bulk, *Angew. Chem. Int. Ed.*, **40**, 1808-1827 (2001).
17. T. R. Dyke, K. M. Mack, and J. S. Muentner, The structure of water dimer from molecular beam electric resonance spectroscopy. *J. Chem. Phys.*, **66**, 498-510 (1977).
18. J. A. Odutola and T. R. Dyke, Partially deuterated water dimers: Microwave spectra and structure, *J. Chem. Phys.*, **72**, 5062-5070 (1980).
19. M. Kobayashi, J. H. Sim, and H. Sato, Conformational analyses for alanine oligomer during hydration by quantum chemical calculation (QCC), *Polym. Bull.*, **74**, 657-670 (2017).

#### Authors

Minoru Kobayashi; Ph.D., Researcher, Graduate School of Bio-Applications and Systems Engineering, Tokyo University of Agriculture and Technology, Tokyo 184-8588, Japan; mikoba3@gmail.com

Jae Ho Sim; Ph.D., Professor, Department of Advanced Materials and Chemical Engineering, Halla University, Wonju 26404, Korea; jhsim@halla.ac.kr